Temperature Feedback Effect Incorporated in HIRE-Theoretic Multigroup Transport Equations

YuGwon Jo and Nam Zin Cho*

Korea Advanced Institute of Science and Technology, 291 Daehak-ro, Yuseong-gu, Daejeon, Korea 34141
**nzcho@kaist.ac.kr*

INTRODUCTION

Homogeneity and isotropy restoration (HIRE) theory has been proposed for a consistent derivation of the multigroup transport equations from the continuous-energy transport equation [1-3]. The HIRE theory maintains angle-independence in the total cross section and homogeneity in a material region (originally each material region is usually homogeneous by design). In addition, only the isotropic moment scattering term remains in the multigroup transport equations.

In the HIRE theory, the partial current discontinuity factor (PCDF) is introduced and it plays a crucial role. To preserve the region-wise neutron leakage, the PCDF is applied at a region interface. The PCDF is initially guessed and iteratively updated by using the Jacobian-Free Newton-Krylov (JFNK) method [4,5].

Recently, the HIRE theory has been applied to a UO_2 pin-cell problem depleted in sub-pin level by Monte Carlo (MC) simulations and successfully reproduced the rim effect in the high burnup UO_2 fuel pin via the multigroup method of characteristics (MOC) calculations [6].

In this paper, the HIRE-theoretic multigroup transport equations are developed under thermal-hydraulic feedback and applied to reproduce the region-averaged fluxes and the k-eigenvalue of the continuous-energy MC simulation for a typical PWR pin-cell problem.

METHODOLOGY

Elements of HIRE Theory and Its PCDFs

We focus on the description of the way to apply the HIRE theory to consider temperature effect in a typical PWR pin-cell problem. The details of the HIRE theory itself is described in Ref. 3. The key idea in the HIRE theory is to replace the traditional definition of the multigroup cross sections, e.g.,

$$\sigma_{t,g}(\vec{r},\vec{\Omega}) = \frac{\int_{E_g}^{E_{g-1}} dE\ \sigma_t(\vec{r},E)\psi(\vec{r},E,\vec{\Omega})}{\int_{E_g}^{E_{g-1}} dE\ \psi(\vec{r},E,\vec{\Omega})}\ , \qquad (1)$$

by

$$\sigma_{t,g}^{m} = \frac{\int_{\vec{r}\in V_m} dV \int d\vec{\Omega}\int_{E_g}^{E_{g-1}} dE\ \sigma_t(\vec{r},E)\psi(\vec{r},E,\vec{\Omega})}{\int_{\vec{r}\in V_m} dV \int d\vec{\Omega}\int_{E_g}^{E_{g-1}} dE\ \psi(\vec{r},E,\vec{\Omega})} \qquad (2)$$

and similarly for other cross sections, with the PCDFs introduced to preserve the region-wise neutron leakage through ∂V_m.

The overall procedure consists of two steps. First, the continuous-energy MC simulation with thermal-hydraulic feedback is performed to generate the parameters for the HIRE theory such as the region-wise cross sections and the net currents at the region interfaces. Then, the multigroup MOC calculations are performed to determine the PCDFs that preserve the region-wise neutron balance and the k_{eff} via iteration. To accelerate the convergence of the PCDFs, the JFNK method with the exponential transformation is applied. Note that the exponential transformation prevents the negative PCDFs, which are unphysical. An overall flow chart for the determination of the PCDFs in the HIRE theory is shown in Fig. 1. In this figure, the PCDFs at iteration l is defined as $\exp(\vec{x}^{(l)})$. If the PCDFs preserve the region-wise neutron balance, $G(\vec{x}^{(l)})$ becomes zero. In practice, the parameters from the MC simulation contain stochastic errors, so the stopping criterion for the PCDF iteration is set as $\left\|G(\vec{x}^{(l)})\right\| < tol$.

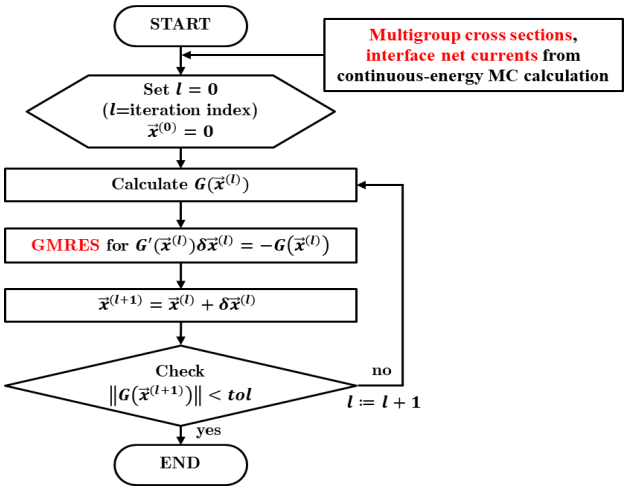

Fig. 1. Flow chart for PCDF iteration in HIRE theory.

Continuous-Energy MC Simulation with Temperature Feedback

The in-house MC code McBOX [7,8] was used for the continuous-energy MC criticality simulation considering temperature effect. The temperature effective cross sections are calculated via the on-the-fly Doppler broadening method based on the refined Gauss-Hermite quadrature [8]. To consider temperature effect in the scattering kernel, the free-gas thermal treatment is applied when $E < 400kT$ or the colliding nuclide is hydrogen [10], where E is the incident neutron energy, k is the Boltzmann constant, and T is the temperature. In the case of U-238, the Doppler broadening rejection correction (DBRC) method [11] is applied when 0.4 eV $< E <$ 210 keV. The stochastic mixing approach for thermal scattering $S(\alpha,\beta)$ data [12] is used in the case of hydrogen bound in water.

At the end of each MC cycle, the region-wise power distributions are obtained by the averaged tallies over the last five MC cycles. Then, the finite difference method is applied to solve the one-dimensional (1-D) cylindrical heat conduction equation, where each region is subdivided into several radial temperature mesh cells to reduce the discretization errors. The volumetric averaged temperature is used to update the temperature in each region for the next MC cycle. At the convergence of both the temperature distributions and the fission source distributions, the HIRE parameters are accumulated during active cycles.

PCDF Iteration via Multigroup MOC Calculations

According to the basics of the HIRE theory, the multigroup transport equations based on the homogenized cross sections alone cannot preserve the region-wise neutron balance in the continuous-energy MC simulation due to the inaccurate region-wise neutron leakage. Thus, the partial currents at the region interfaces are adjusted by the PCDFs during the multigroup transport calculations. The PCDFs that preserve the region-wise neutron balance can be found by the PCDF iteration, as shown in Fig. 1. For that purpose, the in-house multigroup MOC computer code CRX3 [13] was used to perform the PCDF iterations.

NUMERICAL RESULTS

The HIRE theory was tested on the two-dimensional (2-D) UO_2 pin-cell problem with all reflective boundary conditions shown in Fig. 2. To consider temperature effect in details, the UO_2 fuel region was divided into 3 equi-areal radial regions. For the continuous-energy MC simulation, 1,000,000 histories per cycle, 50 inactive cycles, and 400 active cycles were used. The fission source distributions were initially guessed as uniform, while the temperature distributions were initially guessed as 1200 K in UO_2 fuel regions, 900 K in Helium gap, and 900 K in Zircaloy–4. Table I shows the thermal-hydraulic calculational conditions. The temperature-dependent thermal properties of the materials are from Ref. 14 and the steam table from Refs. 15 and 16 were used for the thermal-hydraulic calculation. The average temperature distributions and their standard deviations obtained from 400 active cycles are shown in Table II.

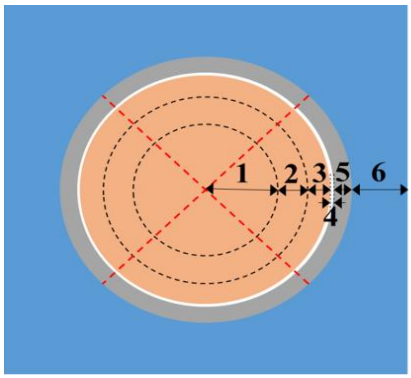

Region Index	Length of Arrow [cm]	Material	Number of Radial Temperature Mesh Cells
1	0.22643	UO_2	5
2	0.09378	UO_2	3
3	0.07197	UO_2	2
4	0.00787	Helium Gap	1
5	0.05715	Zircaloy – 4	1
6	0.17280	Borated Water	1

Fig. 2. Two-dimensional UO_2 pin-cell test problem.

Table I. Thermal-hydraulic calculational conditions

Axial Thermal Power Density	128.87 W/cm
Bulk Coolant Temperature	578.3 K
Coolant Mass Flow Rate	0.315 kg/s

Table II. Average temperature and its standard deviation for each region

Region Index	Average Temperature [K]	Standard Deviation [K]
1	955.7	4.75E-04
2	886.6	1.62E-04
3	822.4	1.54E-05
4	698.5	1.53E-06
5	598.8	0
6	578.3	0

From the continuous-energy MC simulation, the two-group region-wise homogenized cross sections were obtained as in Tables III and IV, while the two-group net currents at region interfaces were obtained in the four out-normal directions, which are distinguished by the red dotted lines in Fig. 2 to take into account for possible extension to arbitrary albedo boundary conditions. The averages of two-group net currents over the four directions are shown in Table V. Note that the energy group boundary was set at 1 eV.

Table III. Two-group total and nu×fission cross sections [cm^{-1}] obtained from continuous-energy MC simulation

Region Index	Fast Group		Thermal Group	
	σ_t	$\nu\sigma_f$	σ_t	$\nu\sigma_f$
1	0.41244	0.02074	0.64149	0.44097
2	0.41615	0.02086	0.64339	0.44510
3	0.43533	0.02103	0.64596	0.45037
4	0.00049	0.00000	0.00020	0.00000
5	0.32279	0.00000	0.31012	0.00000
6	0.64175	0.00000	1.73869	0.00000

Table IV. Two-group scattering cross sections [cm^{-1}] obtained from continuous-energy MC simulation

Region Index	$\sigma_{s,1\to1}$	$\sigma_{s,1\to2}$	$\sigma_{s,2\to1}$	$\sigma_{s,2\to2}$
1	0.38632	0.00076	0.00091	0.39847
2	0.38858	0.00076	0.00083	0.39822
3	0.39788	0.00076	0.00075	0.39807
4	0.00049	0.00000	0.00000	0.00020
5	0.32084	0.00033	0.00047	0.30547
6	0.61168	0.02952	0.00064	1.71516

Table V. Average of two-group net currents [#/cm^2·sec] over four directions at region interfaces obtained from continuous-energy MC simulation

Region Index	Fast Group	Thermal Group
1	1.28093E+12	-9.67705E+11
2	1.82183E+12	-1.38869E+12
3	2.14702E+12	-1.73034E+12
4	2.10477E+12	-1.69629E+12
5	1.82278E+12	-1.49055E+12
6	0.00000E+00	0.00000E+00

To find the PCDFs, the two-group MOC calculations were performed with the following conditions: 56 radial mesh cells (6 ring divisions and 8 azimuthal sector divisions) per modular fuel pin cell, and 8 azimuthal × 3 polar angles per octant with 150 rays per cell per angle. The relative norm error criterion was 10^{-8} for the fission source. In the PCDF iteration, the error criterion for the PCDFs was set to 10^{-6}. The number of PCDF iterations with the JFNK method was 2, where the number of MOC calculation was 82. Table VI shows the average of converged two-group PCDFs over the four directions at region interfaces.

Table VI. Average of converged two-group PCDFs over four directions at region interfaces

Region Index	Fast Group		Thermal Group	
	Outward PCDF	Inward PCDF	Outward PCDF	Inward PCDF
1	1.00107	0.99896	0.99911	1.00099
2	0.99872	1.00123	0.99990	1.00012
3	0.99863	1.00132	0.99979	1.00025
4	0.99892	1.00103	1.00000	1.00000
5	0.99996	1.00004	1.00175	0.99795
6	1.00000	1.00000	1.00000	1.00000

Table VII and Fig. 3 show the multiplication factor and the flux distributions, respectively, obtained from the HIRE theoretic two-group MOC calculations. The error in the multiplication factor k_{eff}^{HIRE} is 3.8 pcm, which is smaller than the standard deviation in the multiplication factor from the reference MC simulation k_{eff}^{MC} . The maximum relative errors in the fast and thermal flux distributions are 0.64% and 0.7%, respectively, which occur in the helium gap.

Table VII. Multiplication factor obtained from the two-group HIRE-theoretic MOC calculation

k_{eff}^{MC} (standard deviation)	k_{eff}^{HIRE}	$k_{eff}^{MC} - k_{eff}^{HIRE}$
1.211777 (4.2 pcm)	1.211808	3.8 pcm

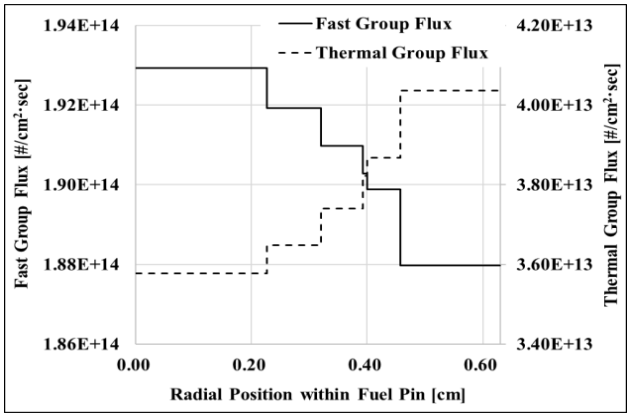

Fig. 3. Fast group flux distributions (left axis) and thermal group flux distributions (right axis) obtained from the two-group HIRE-theoretic MOC calculations.

CONCLUDING REMARKS

In this paper, the HIRE theory was applied to the 2-D UO_2 pin-cell problem to consider the temperature effect in the reactor analysis. From the continuous-energy MC simulation with temperature feedback via the simple thermal-hydraulic calculation, the region-wise homogenized cross sections and net currents at region interfaces were generated. The HIRE-theoretic two-group MOC calculations with the PCDF iterations gave the accurate k_{eff} and two-group flux distributions. This indicates that only a few group (instead of a very fine group) representation may be allowed in advanced reactors design analysis.

For the practical application of the HIRE theory to the whole-core multigroup transport calculation, a study for tabulation or functionalization of the HIRE parameters (homogenized cross sections and PCDFs) in albedo, depletion, and temperature is needed for a set of typical "unit" problems (this could be assisted by multi-variate linear interpolation methods or various artificial intelligence techniques). The unit problem can be, typically, a fuel pin cell in light water reactors (LWRs), or a fuel assembly in fast breeder reactors (FBRs). Then, the unit problems will "tile and pile" the whole-core, that will be submitted for the HIRE multigroup transport calculations, as outlined in Ref. 3.

ACKNOWLEDGEMENTS

The authors wish to thank Seungsu Yuk now of Korea Atomic Energy Research Institute (KAERI) for useful discussions and help to use the CRX3 code. This work was supported in part by a National Research Foundation grant funded by Ministry of Science, ICT and Future Planning of the Republic of Korea (No. 2015M2B2A9029928).

REFERENCES

1. Y.G. JO and N. Z. CHO, "Homogeneity and Isotropy Restoration Theory for Derivation of Multigroup Transport Equation," *Trans. Kor. Nucl. Soc.*, Jeju, Korea, May 12-13, 2016, Korean Nuclear Society (2016).

2. N. Z. CHO, Y.G. JO, and S. YUK, "Multigroup Transport Equations Derived via Homogeneity and Isotropy Restoration Theory," *Trans. Am. Nucl. Soc.*, **115**, 592-595 (2016).

3. N. Z. CHO, Y.G. JO, and S. YUK, "A New Derivation of the Multigroup Transport Equations via Homogeneity and Isotropy Restoration Theory," *Ann. Nucl. Energy*, **110**, 798-804 (2017).

4. D. A. KNOLL, and D. E. KEYES, "Jacobian-Free Newton-Krylov Methods: A Survey of Approaches and Applications," *J. Comp. Physics*, **193**, 357 (2004).

5. H. PARK, et al., "Nonlinear Acceleration of Transport Criticality Problems," *Nucl. Sci. Eng.*, **172**, 52 (2012).

6. Y.G. JO, N. Z. CHO, and S. YUK, "Depletion Rim Effect Incorporated in HIRE-Theoretic Multigroup Transport Equations," *Trans. Am. Nucl. Soc.*, **117**, 1436-1439 (2017).

7. Y.G. JO, "Study of New Features and Their Implementations in the Nuclear Reactor Analysis Monte Carlo Code – McBOX," Ph.D. Thesis, KAIST, 2017.

8. Y.G. JO and N. Z. CHO, "User's Manual for McBOX – A Monte Carlo Code Version 1," Korea Advanced Institute of Science and Technology, NURAPT-2016-03 (April 2016).

9. JO and N. Z. CHO, "Refinements of On-the-Fly Doppler Broadening via Gauss-Hermite Quadrature in Monte Carlo Reactor Analysis," *Trans. Kor. Nucl. Soc.*, Jeju, Korea, May 18-19, 2017.

10. X-5 MONTE CARLO TEAM, "MCNP – A General N-Particle Transport Code, Version 5 – Volume I: Overview and Theory", LA-UR-03-1987, Los Alamos National Laboratory (April 2003).

11. B. BECKER, et al., "Proof and implementation of the stochastic formula for ideal gas, energy dependent scattering kernel," *Ann. Nucl. Energy*, **36**, 470-474 (2009).

12. T. VIITANEN and J. LEPPÄNEN, "New Interpolation Capabilities for Thermal Scattering Data in SERPENT 2," PHYSOR 2016, Sun Valley, ID, USA, May 1-5, 2016.

13. S. YUK and N. Z. CHO, "User's Manual for the Method of Characteristics Computer Code Package CRX3 Version 1.0," Korea Advanced Institute of Science and Technology, NURAPT-2017-01 (February 2017).

14. IAEA, "Thermophysical properties database of materials for light water reactors and heavy water reactors," IAEA-TECDOC-1496 (2006).

15. L. HAAR, et al., "NBS/NRC Steam Tables: Thermodynamic and Transport Properties and Computer Programs for Vapor and Liquid States of Water in SI Units," Hemisphere Publishing Corporation, Washington, 1984.

16. C. A. MEYER, et al., "ASME Steam Tables: Thermodynamic and Transport Properties of Steam," American Society of Mechanical Engineers, Fifth Edition, 1983.